Forward Problem of Three Dimensional EIT in Thorax Model

Huanli Wu, Guizhi Xu, Shuai Zhang, Shuo Yang, Ying Li, and Weili Yan

***Abstract*—The forward problem of the three dimensional electrical impedance tomography is presented in thorax model. Here potential distribution on the edge of the model measuring plan can be gotten by finite element method. The potential distributions of inhaling and exhaling models are shown, and the opposite drive pattern are adopted with single drive current or multiple drive current. The forward problem is the base of the inverse problem in EIT research, and it is helpful to the monitor on thorax activities.**

I. Introduction

ELECTRICAL impedance tomography (EIT) is a technique for determining the impedance distribution of the inner body by measuring on the surface, and it is to find whether some pathology has happened or some activity is happening by monitoring the impedance change in the special tissue. EIT has previously been restricted to the assumption that the data originate from a two dimensional (2D) object. In practice, the object is generally a three dimensional (3D) structure, and thus the injected current will flow not only within the measurement plane but also through the off-plane volume. The 3D EIT is a better method in order to get more accurate data in experiments.

Some new methods in EIT have been put forward, for example, the Bayesian Markov chain Monte Carlo (MCMC) approach [1] and the preconditioned conjugate gradients (PCGs) algorithm [2]. However, the traditional method finite element method (FEM) has its own merits. For example, it has the advantage of computing any shape of object and handling the inhomogeneous object. The numerical solution of the EIT can be gotten easily by FEM. This method has been widely used previously [3-5].

The forward problem of 3D EIT in the thorax model is introduced in this paper, and the potential distributions are given while the thorax inhaling and exhaling. The potential distributions are gotten by FEM. The node potential on the edge of the measuring plane changes not only with the activities in the thorax model, but also with the drive patterns. Obiter, each thorax model is supposed to be a column having unit height and unit radius.

This work is supported by the Natural Science Foundation of Tianjin City 06YFJMJC11000 and the Natural Science Foundation of Hebei Province E2005000047.

Huanli Wu is with the Province-Ministry Joint Key Laboratory of Electromagnetic Field and Electrical Apparatus Reliability, Hebei University of Technology, Tianjin 300130, China. (e-mail: hlwu2003@126.com).

Guizhi Xu, Shuai Zhang, Shuo Yang, Ying Li, and Weili Yan are with the Province-Ministry Joint Key Laboratory of Electromagnetic Field and Electrical Apparatus Reliability, Hebei University of Technology, Tianjin 300130, China.

II. Math Equations

The forward problem of EIT is to find the potential (Φ) arising from the injected current-carrying electrodes onto the special object. The mathematical model is the following Laplace equation with the given boundary conditions,

$$\nabla \cdot \sigma \nabla \Phi = 0 \tag{1}$$

Neumann boundary condition,

$$\sigma \frac{\partial \Phi}{\partial n} = -J \tag{2}$$

where σ is the conductivity and J is the injected current density. FEM is adopted here to solve the forward problem of the three dimensional EIT.

The equivalent variation of Laplace equation (1) is

$$F(\Phi) = -\frac{1}{2}\int_v \Phi \nabla \cdot \sigma \nabla \Phi \, dv = \min \tag{3}$$

III. Forward Problem of Thorax in Eit

A. Subdivision of the cylinder model

The cylinder model is used in the forward problem of 3D EIT, which is looked on as the thorax of human in this paper. Fig.1 shows the surface figure which is gotten by subdividing the cylinder model with triangular prism. The cylinder model is subdivided into 4608 elements with 2817 nodes. The drive current is used to the opposite drive electrodes during calculating the node potential with FEM. Positions of the drive electrodes are (1, 0, 0.5) and (-1, 0, 0.5) when adding electrodes onto the surface of the cylinder model. In fact, the cylinder is subdivided into eight levels, and each of them has 576 elements.

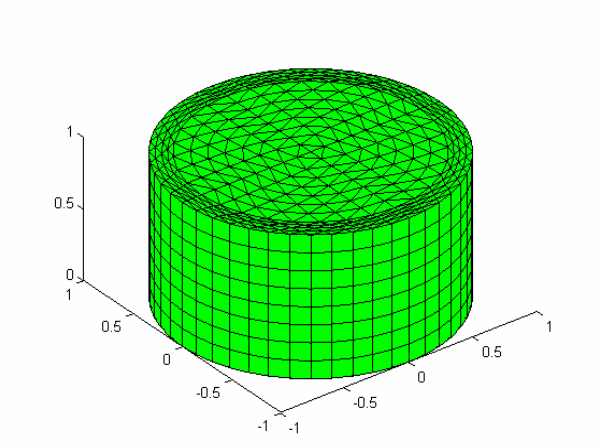

Fig. 1. Cylinder model.

B. Finite element discretization

As is described in [5],

$$K\Phi^{T} = Q \tag{4}$$

where $K = [K_{ij}]$ is the coefficient matrix, which is superposed by the coefficient of all elements. It can be written as $K_{ij} = \sum_{e=1}^{e_0} K_{ij}^{e}$, where e_0 is the total amount of the elements. Φ is the node potential matrix and Q is the excitation matrix contributed by the injected current.

In this paper, the triangular prism shown in Fig.2 is used. For the element e, the potential function given below is adopted to determine the potential Φ^{e} on each element as follows:

$$\Phi^{e}(x,y,z) = a + bx + cy + dz + exz + fyz \tag{5}$$

where a, b, c, d, e and f are constants, x, y, and z are coordinates. Assuming the coordinates of nodes K, M, N, K', M' and N' are (x_K, y_K, z_K), (x_M, y_M, z_M), (x_N, y_N, z_N), $(x_{K'}, y_{K'}, z_{K'})$, $(x_{M'}, y_{M'}, z_{M'})$, and $(x_{N'}, y_{N'}, z_{N'})$. Then

$$\begin{cases} x_K = x_{K'} & y_K = y_{K'} \\ x_M = x_{M'} & y_M = y_{M'} \\ x_N = x_{N'} & y_N = y_{N'} \end{cases} \tag{6}$$

The potential of each node in the element of the triangular prism should be

$$\Phi_j(x,y,z) = a + bx_j + cy_j + dz_j + ex_jz_j + fy_jz_j \tag{7}$$

Assuming that

$p_K = x_M y_N - y_M x_N$, $p_M = x_N y_K - y_N x_K$, $p_N = x_K y_M - y_K x_M$, $q_K = y_M - y_N$, $q_M = y_N - y_K$, $q_N = y_K - y_M$, $r_K = x_N - x_M$, $r_M = x_K - x_N$, $r_N = x_M - x_K$, $h = z' - z$, *and* $z' > z$, then the coefficients in equaption (7) are

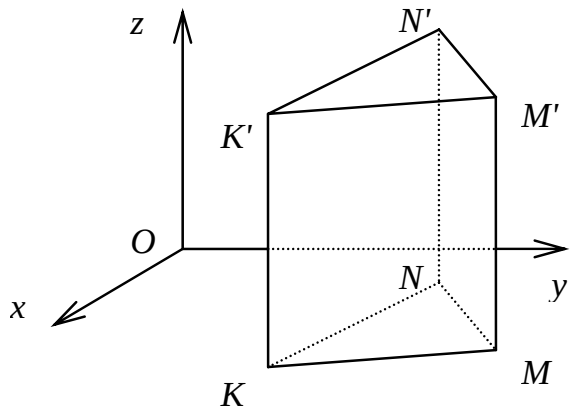

Fig. 2. Triangular prism element used for FEM mesh

$$a = \frac{1}{4\Delta}\left[\left(1+\frac{s}{h}\right)\left(p_K\Phi_K + p_M\Phi_M + p_N\Phi_N\right) + \left(1-\frac{s}{h}\right)\left(p_K\Phi_{K'} + p_M\Phi_{M'} + p_N\Phi_{N'}\right)\right],$$

$$b = \frac{1}{4\Delta}\left[\left(1+\frac{s}{h}\right)\left(q_K\Phi_K + q_M\Phi_M + q_N\Phi_N\right) + \left(1-\frac{s}{h}\right)\left(q_K\Phi_{K'} + q_M\Phi_{M'} + q_N\Phi_{N'}\right)\right],$$

$$c = \frac{1}{4\Delta}\left[\left(1+\frac{s}{h}\right)\left(r_K\Phi_K + r_M\Phi_M + r_N\Phi_N\right) + \left(1-\frac{s}{h}\right)\left(r_K\Phi_{K'} + r_M\Phi_{M'} + r_N\Phi_{N'}\right)\right],$$

$$d = \frac{1}{2\Delta}\left(\frac{\Phi_{K'}-\Phi_K}{h}p_K + \frac{\Phi_{M'}-\Phi_M}{h}p_M \frac{\Phi_{N'}-\Phi_N}{h}p_N\right),$$

$$e = \frac{1}{2\Delta}\left(\frac{\Phi_{K'}-\Phi_K}{h}q_K + \frac{\Phi_{M'}-\Phi_M}{h}q_M \frac{\Phi_{N'}-\Phi_N}{h}q_N\right),$$

$$f = \frac{1}{2\Delta}\left(\frac{\Phi_{K'}-\Phi_K}{h}r_K + \frac{\Phi_{M'}-\Phi_M}{h}r_M \frac{\Phi_{N'}-\Phi_N}{h}r_N\right).$$

After analyzing of the element, K_{ij}^{e} is as following:

$$K_{ij}^{e} = \sigma^{e}\left[\frac{h}{16\Delta}\left(1+\frac{\zeta_i\zeta_j}{3}\right)q_iq_j + \frac{h}{16\Delta}\left(1+\frac{\zeta_i\zeta_j}{3}\right)r_ir_j\right] + \begin{cases} \sigma^{e}\dfrac{\zeta_i\zeta_j\Delta}{16h} & (j = i \ \ or \ \ i') \\ \sigma^{e}\dfrac{\zeta_i\zeta_j\Delta}{12h} & (j \neq i \ \ or \ \ i') \end{cases} \tag{8}$$

where $i = K, M, N, K', M', N'$, and $\zeta_i = \begin{cases} -1, & (i = K, M, N) \\ 1, & (i = K', M', N') \end{cases}$. If Q is known, then node potential of the cylinder can be gotten.

IV. Solutions of the Thorax Models

Here some kinds of cylinders are used as the thorax models. They are homogeneous model, inhomogeneous, and the inhaling and exhaling models. The same drive current, which is 1*mA*, is used in these three models in order to improve the credence. And the drive electrodes are placed on the same place which is in the median plane of the cylinder when only one single drive patter is used. The input electrode is placed on the place (1, 0, 0.5) and the output electrode is placed on the place (-1, 0, 0.5) in the single drive current pattern. They are on the opposite positions, so this pattern is called opposite drive. The resistivity is $1\ \Omega \cdot m$ in the homogeneous model. The resistivity of most elements is $1\ \Omega \cdot m$ in the inhomogeneous model, but the element which is in the center of the cylinder is $5\ \Omega \cdot m$. Fig.3 shows node potentials (*mV*) on the edge of the plane on the bottom of the

homogeneous and inhomogeneous models. The solid line is the potential distribution of the homogeneous model and the star line is the one of the inhomogeneous model. The absolute value of the node potential becomes lower and lower when the distance becomes more and more further from the drive electrode, whereas, it becomes higher when the distance is nearer and nearer to the driver electrode. The difference between the two lines is that the absolute value of the node potential in the inhomogeneous model is higher than that in the homogeneous one. Then we can draw such a conclusion that the change of the inner resistivity can provoke the variation of potential on the object surface.

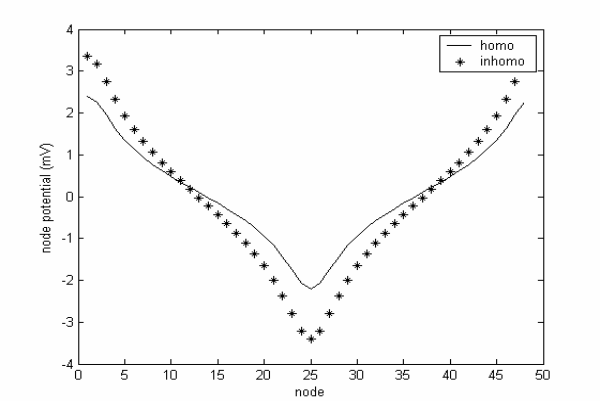

Fig. 3. Node potentials of the homogeneous and inhomogeneous models.

The inhaling thorax model is shown in Fig.4, and most of the elements have the same resistivity as $1\,\Omega \cdot m$, but the inner ones marked with different color have the resistivity of $5\,\Omega \cdot m$. The node potential of the inhaling thorax model with single drive current pattern is shown in Fig.5. While adopting multiple drive currents pattern, one is above the middle plane and the other is below it, the node potential distribution is shown in Fig.6. The potential is larger in the multiple drive currents pattern than that in the single drive current pattern.

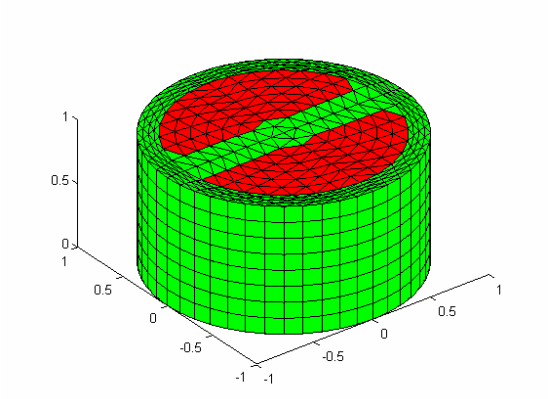

Fig. 4. The inhaling thorax model.

The exhaling thorax model is shown in Fig.7. Most elements have the resistivity of $1\,\Omega \cdot m$, and the marked elements with different color have the resistivity of $5\,\Omega \cdot m$.

The node potential is shown in Fig.8 with the single drive current pattern. If multiple drive currents pattern is used, the node potential is shown in Fig.9. In order to find the difference of the inhaling and exhaling thorax models, the potential distributions of these two models with single drive pattern are drawn in one figure-Fig.10. It is proved that the absolute value of the potential becomes lower when the activities of the thorax change from inhaling to exhaling because of the resistivity change.

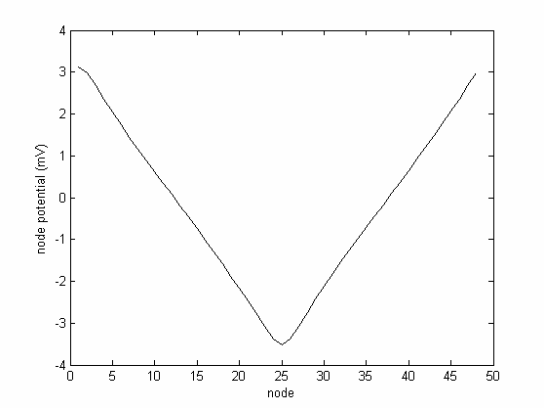

Fig. 5. Node potentials of the inhaling thorax model with single drive current pattern.

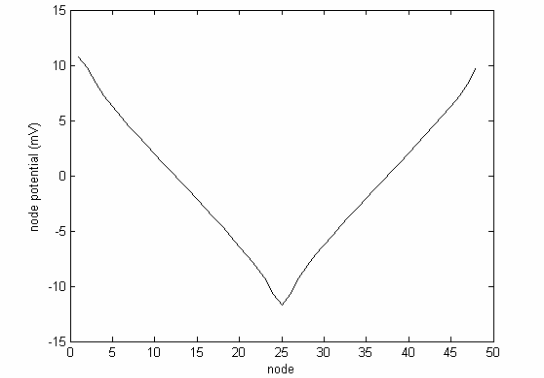

Fig. 6. Node potentials of the inhaling thorax model with multiple drive currents pattern.

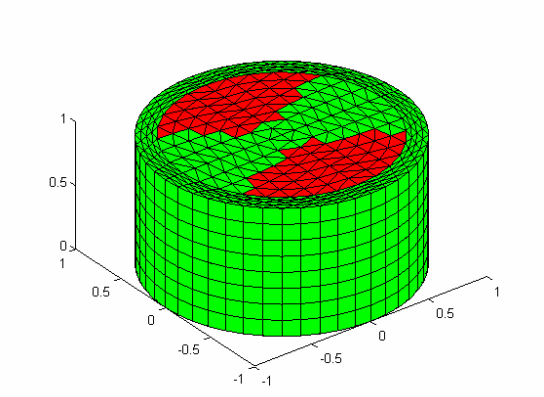

Fig. 7. The exhaling thorax model.

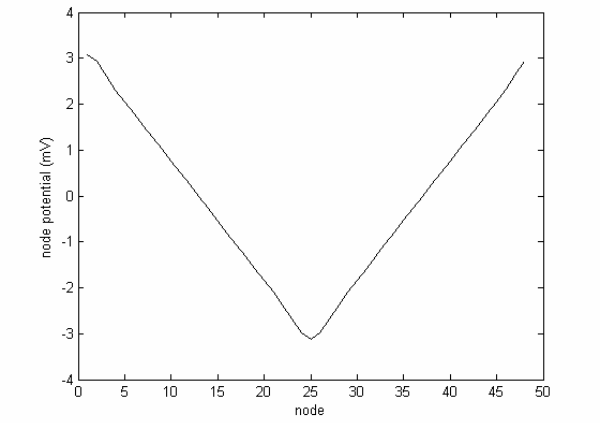

Fig. 8. Node potentials of the exhaling thorax model with single drive current pattern.

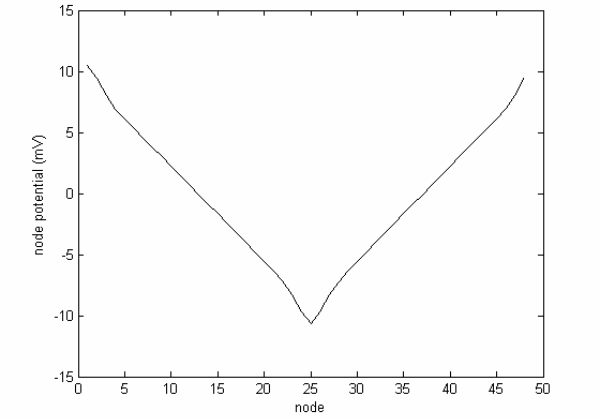

Fig. 9. Node potentials of the exhaling thorax model with multiple drive currents pattern.

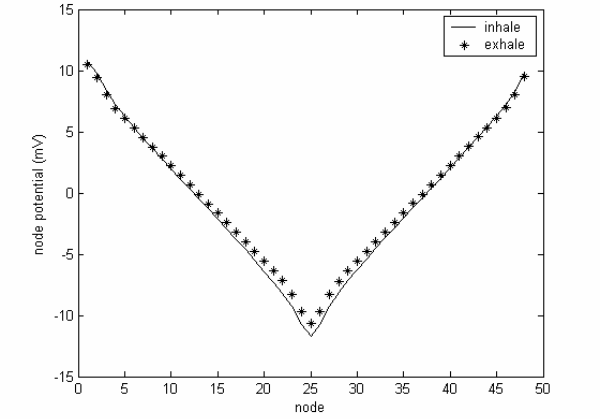

Fig. 10. Node potentials of the inhaling and exhaling thorax model with multiple drive currents pattern.

V. Conclusion

In the forward problem of the thorax model, the node potentials on the edge of the cylinder can indicate the change of the resistivity in the inner of it. In this paper, the potential distributions of nodes on the edge of the measuring plane are described while inhaling and exhaling. It is shown that the potentials change with the change of the thorax activities. Therefore, it is helpful to judge if there are any physiological activities and pathologic changes in the special object. Multiple drive currents pattern is used in this paper, and it is helpful to improve the node potential.

VI. Further Work

The forward problem in 3D EIT is the primary stage of the research in EIT. The inverse problem based on it will be the first importance work in the future. With the help of the research in the inverse problem, we can determine the impedance distribution in the special tissue. Then we can judge which activity has happened in the special tissue because that different activities can lead to different changes of impedance, such as, inhaling and exhaling.

Although there are several algorithms have been used in the inverse problem in 3D EIT, but the best algorithm is to be discovered in the inverse problem. Therefore, to find a more suitable algorithm in the inverse problem is a primate task in the further work.

References

[1] R. G. Aykroyd, B. A. Cattle and R. M. West, “Boundary element method and markov chain monte carlo for object location in electrical impedance tomography,” Proceedings of the 5th International Conference on Inverse Problems in Engineering: Theory and Practice, Cambridge, UK, 11–15th July 2005.

[2] N. Polydorides, W. R. B. Lionheart and H. McCann. “Krylov subspace iterative techniques: on the detection of brain activity with electrical impedance tomography,” IEEE Trans. on Med. Imaging, Vol. 21, No.6, June 2002. pp. 596–603.

[3] F. Lin, B. Moran, J. Bankard, R. Hendrix, and M. Makhsous. “A subject-specific FEM model for evaluating buttock tissue response under sitting load,” Proceedings of the 26th Annual International Conference of the IEEE EMBS San Francisco, CA, USA • September 1-5, 2004, pp. 5088–5091.

[4] B. Katyal and P. H. Schimpf. “Multiple Current Dipole Estimation in a Realistic Head Model Using R-MUSIC,” Proceedings of the 26th Annual International Conference of the IEEE EMBS San Francisco, CA, USA • September 1-5, 2004, pp.829–532.

[5] G. Z. Xu, H. L. Wu, S. Yang, et al. “3-D Electrical Impedance Tomography Forward Problem With Finite Element Method,” IEEE Transactions on Magnetics ,Vol. 41, No.5, May 2005, pp1832–1835.